Updates of Some Standard EM Models

Mihály Novák
CERN (EP-SFT)

28-08-2018

Contents

Contents

Before (more details can be found here) :

- a new version of the Goudsmit-Saunderson multiple Coulomb scattering model was developed (3 years ago, Geant4.10.2)
- employs exact Goudsmit-Saunderson angular distributions
- based on (relativistic) screened-Rutherford elastic DCS (DCS_{SRF}): scattering of **spinless** e^- on **exponentially screened**, **point** like Coulomb **potential**
- solution of the relativistic Schrödinger equation (Klein-Gordon equation) for spinless $e^-(/e^+)$ under the first Born approximation
- simple analytical DCS with only one screening parameter $\rightarrow$ smooth transformed GS angular distributions $\rightarrow$ very efficient sampling of angular deflection
- this model was developed by Kawrakow and Bielajew[1] (the EGSnrc one)
- the new Geant4 GS model was significantly faster, more robust and theoretically more consistent compared to the previous version ($<$ Geant4.10.2)

[1] I.Kawrakow,A.F.Bielajew, NIMB 134(1998)325-336]

With Geant4.10.4: Mott or spin-relativistic corrections:

- Mott DCS (DCS_{Mott}): scattering of e^-/e^+ **with spin** on a point like, unscreened Coulomb potential (the unscreened Rutherford DCS is the spinless correspondence)
- solution of the Dirac equation with a point like, unscreened scattering potential: relativistic Dirac-Coulomb partial wave calculation
- the DCS used is

$$\frac{d\sigma}{d\Omega} = \frac{d\sigma}{d\Omega}(Z, E_{kin}, \theta) = \left[\frac{ZZ'e^2}{pc\beta}\right]^2 \frac{R_{Mott}(Z, E_{kin}, \theta)}{[1-\cos(\theta)+\eta']^2} \equiv \text{DCS}_{SRF\times Mott}$$

  - where $R_{Mott}(Z, E_{kin}, \theta) = \text{DCS}_{\text{Mott}}/\text{DCS}_{\text{RF}}$ with DCS_{RF} being the unscreened, relativistic Rutherford DCS
  - η' is a modified screening parameter such that the most accurate PWA first transport cross section (that determines the mean of the GS angular distribution) is reproduced by $\text{DCS}(\eta')_{SRF\times Mott}$ i.e. the solution of

$$2\pi\int_0^{\pi}[1-P_{l=1}(\cos(\theta))]\frac{d\sigma}{d\Omega}\sin\theta d\theta = 2\pi\int_0^{\pi}[1-P_{l=1}(\cos(\theta))]\frac{d\sigma}{d\Omega}^{PWA}\sin\theta d\theta$$

- GS angular distributions were computed based on this form of the DCS and the corresponding rejection functions are stored in files

Theoretical background (in a nutshell)

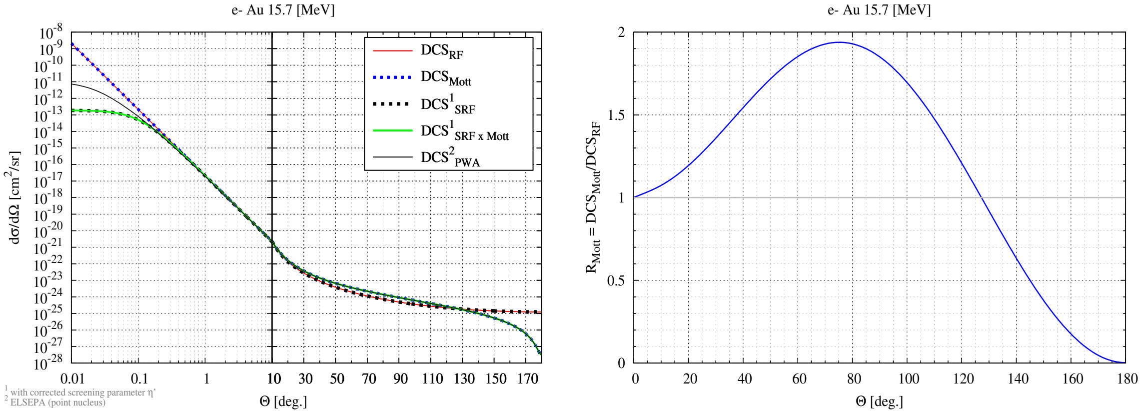

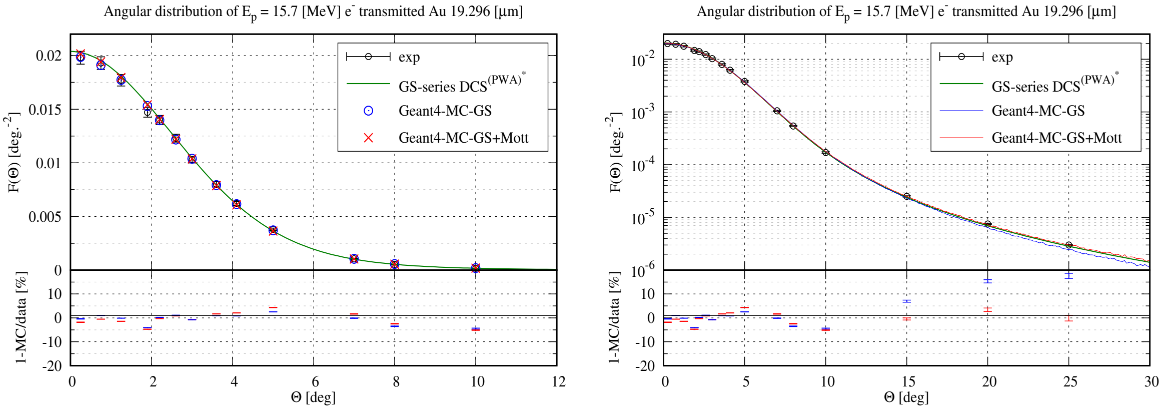
Angular distribution of E_p = 15.7 [MeV] e^- transmitted Au 19.296 [µm]
exp
GS-series DCS$^{(PWA)*}$
Geant4-MC-GS
Geant4-MC-GS+Mott
F(Θ) [deg.$^{-2}$]
1-MC/data [%]
Θ [deg]
Angular distribution of E_p = 15.7 [MeV] e^- transmitted Au 19.296 [µm]
exp
GS-series DCS$^{(PWA)*}$
Geant4-MC-GS
Geant4-MC-GS+Mott
F(Θ) [deg.$^{-2}$]
1-MC/data [%]
Θ [deg]

Contents

More results: SANDIA depth dose data (**left:** Geant4.10.4 vs data; **right:** EGSnrc vs data)

Mott correction makes the shower longer/shorter for low-Z/high-Z materials.

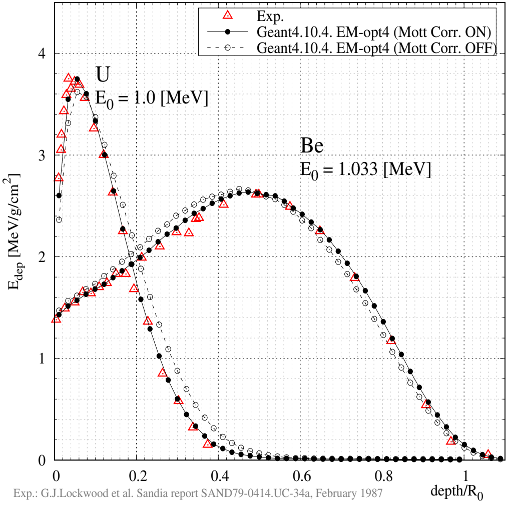

Exp.: G.J.Lockwood et al. Sandia report SAND79-0414.UC-34a, February 1987

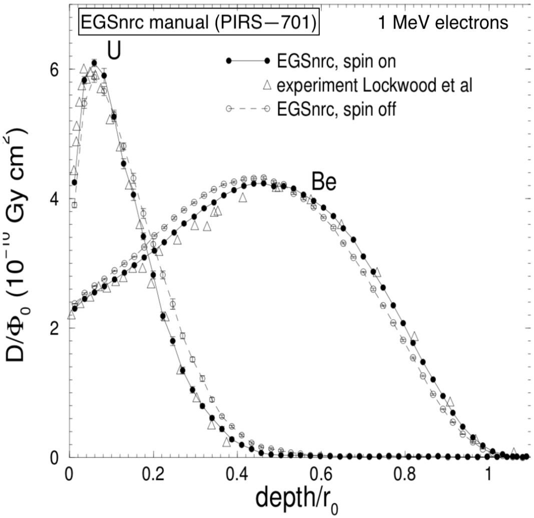

More results: SANDIA depth dose data (**left:** Geant4.10.4 vs data; **right:** EGSnrc vs data)

Even EM-option GS (opt0 with GS-MSC) can describe the data with proper MSC settings.

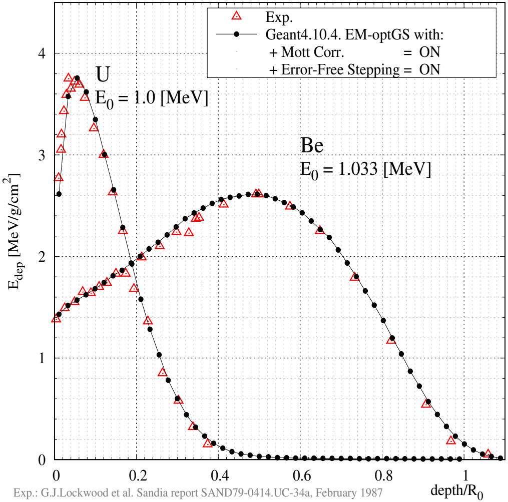

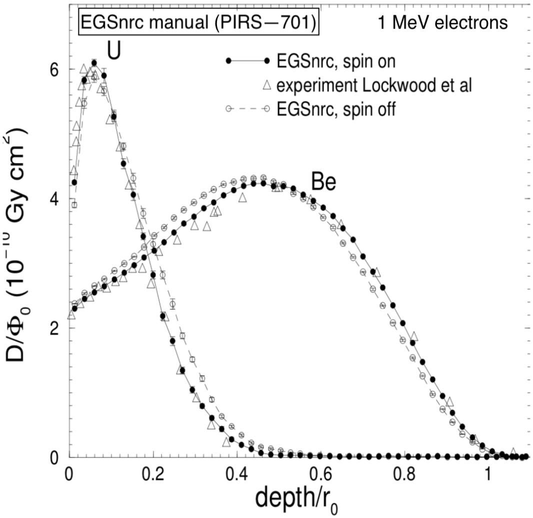

More results: low energy e^- in water, Dose Point Kernel simulation was a long standing problem (**Geant4.10.5.beta vs EGSnrc**)

EGSnrc doesn't have model for energy loss straggling!

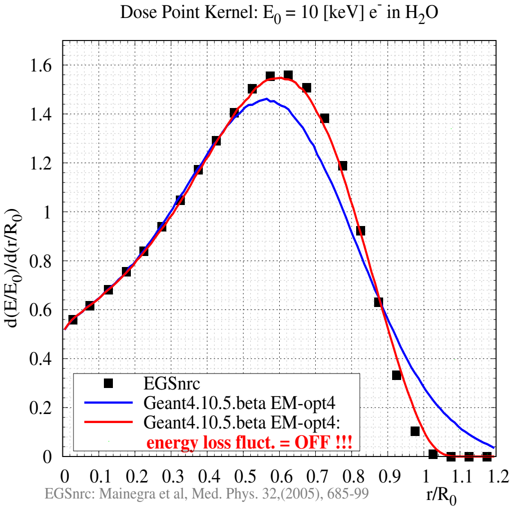

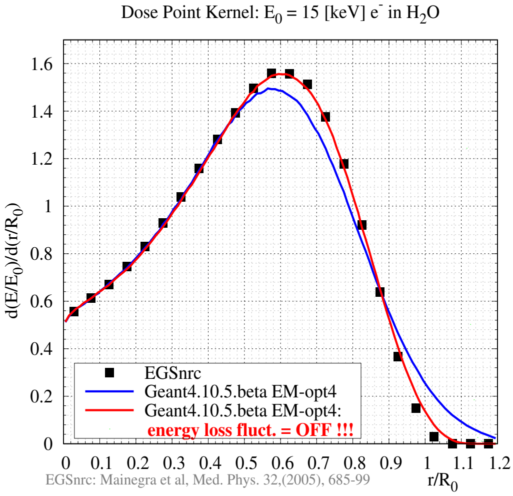

More results: low energy e^- in Silicon, depth dose data (**left:** Geant4.10.5.beta vs data; **right:** PENELOPE vs data)

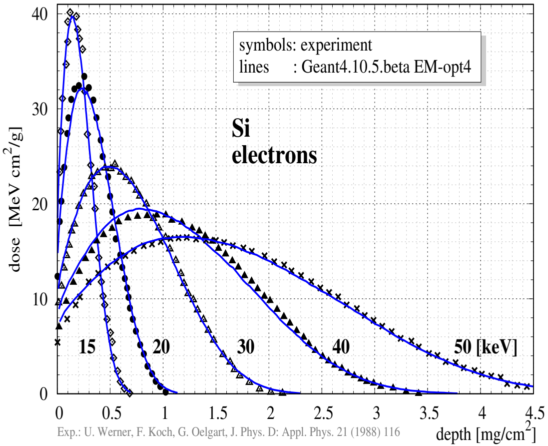

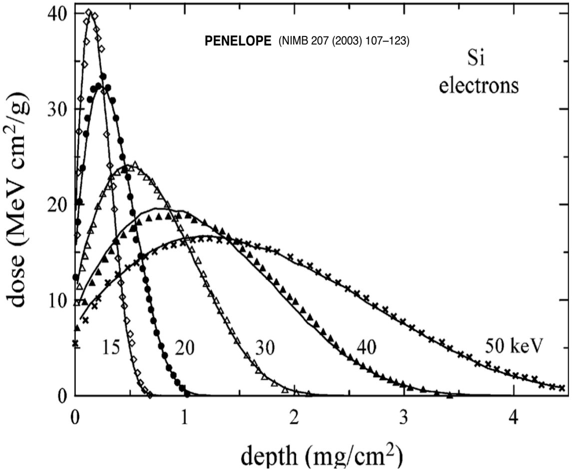

More results: e^- backscattering, Geant4.10.5.beta vs data, EGSnrc, PENELOPE (**left:** Al; **right:** Au)

EGSnrc: based on E.S.M.Ali and D.W.O. Rogers, Phys. Med. Biol. 53 (2008) 1527-1543

PENELOPE: J.Sempau et al. Nucl. Instr. and Meth. in Phys. Res. B 207(2003)107-123

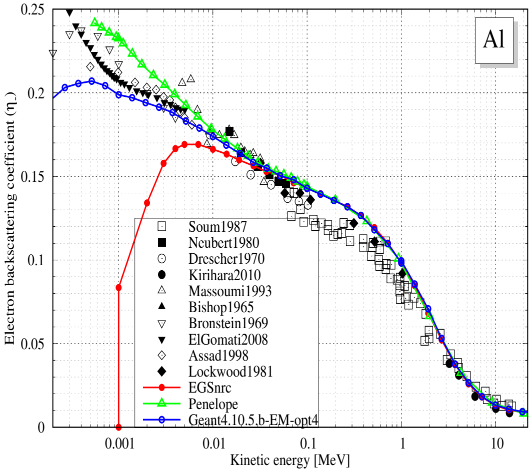

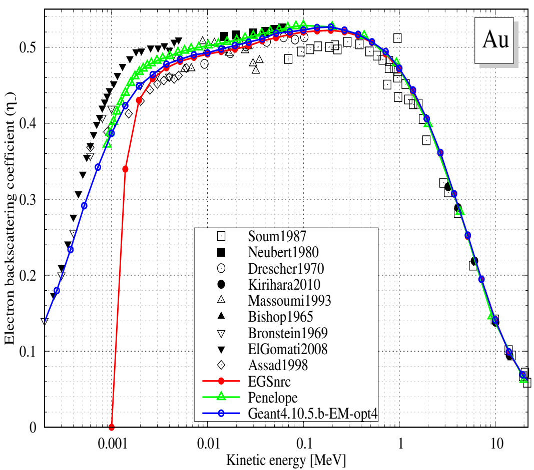

More results: e^- backscattering (**left:** Geant4.10.5.beta vs data; **right:** EGSnrc vs data)

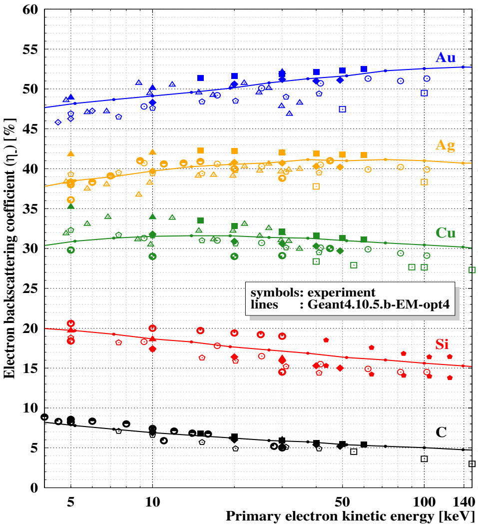

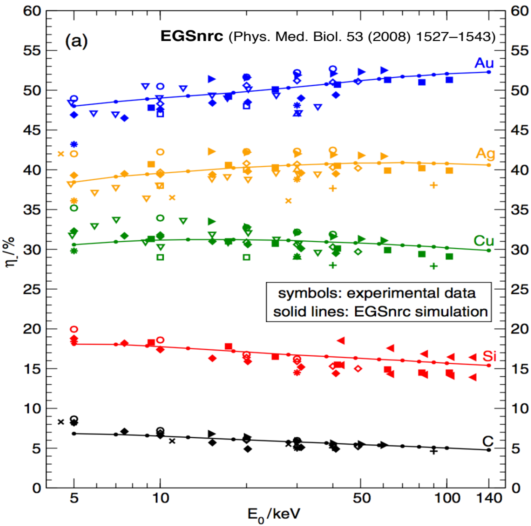

More results: e⁻ backscattering (**left:** Geant4.10.5.beta vs data; **right:** EGSnrc vs data)

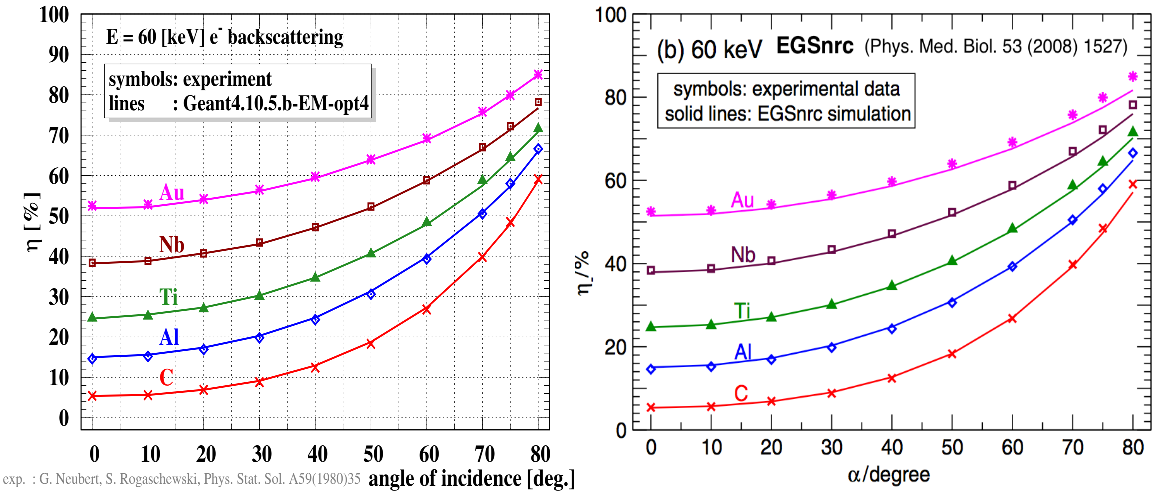

GS-Mott conclusion:

- the Geant4 Goudsmit-Saunderson MSC model has settings (version $\geq$ Geant4-10.4.) to describe $e^{-/+}$ transport with high accuracy from low to high Z materials down to $\sim$ keV energies
- in order to demonstrate this, a very detailed $e^{-/+}$ transport benchmark is ongoing: comparing simulated (any and many type of) experimental data:
  - backscattering/transmission coefficients, energy/angular distributions, depth dose
  - wide range of primary energy: form few hundred eV up to few tens of MeV
  - from low to high Z materials
- see more on these results at: **3rd Geant4 International User Conference at the Physics-Medicine-Biology Frontier, Bordeaux (France), 29-31 October 2018**

Contents

Contents

G4BetheHeitlerModel and G4PairProductionRealModel

- both model final state sampling is based on the Bethe-Heitler DCS[1] (with screening and Coulomb corrections and including conversion in the field of atomic electrons)
- the low-energy model (`G4BetheHeitlerModel`) employs parameterised cross section while the high energy model (`G4PairProductionRealModel`), that includes LPM suppression, makes use of numerically integrated cross sections
- screening correction is introduced through screening functions based on the Thomas-Fermi(TF) model of the atom (Butcher-Messel[2] analytical approximation)
- complete screening approximation is used, with *radiation logarithms* computed from the "Hartree-Fock" model of the atom, for low Z atoms where the TF model doesn't work (see more on this later)

---

[1] H Bethe, W Heitler - Proc. R. Soc. Lond. A, 1934

[2] J. C. Butcher and H. Messel - Nuclear Physics, vol. 20, pp. 15?128, 196

Some artificial structures can be observed in the e^-/e^+ energy distributions

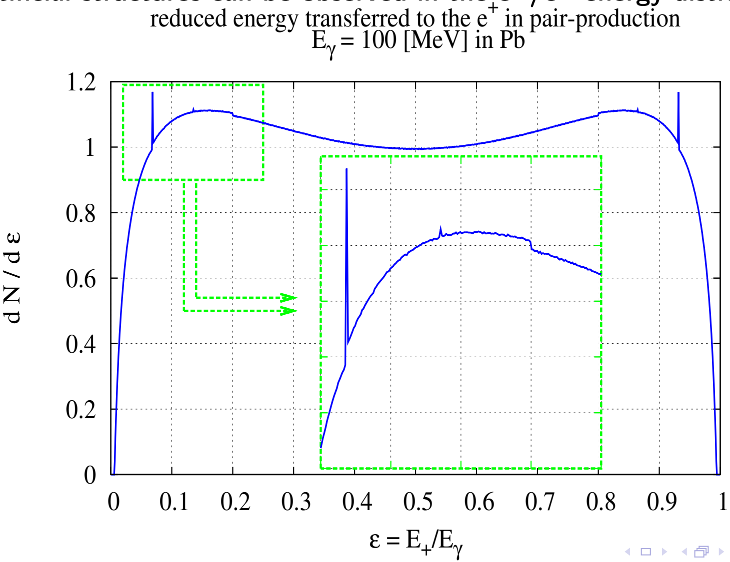

"Spikes" has been removed by improving the `G4Pow::A13` approximation.

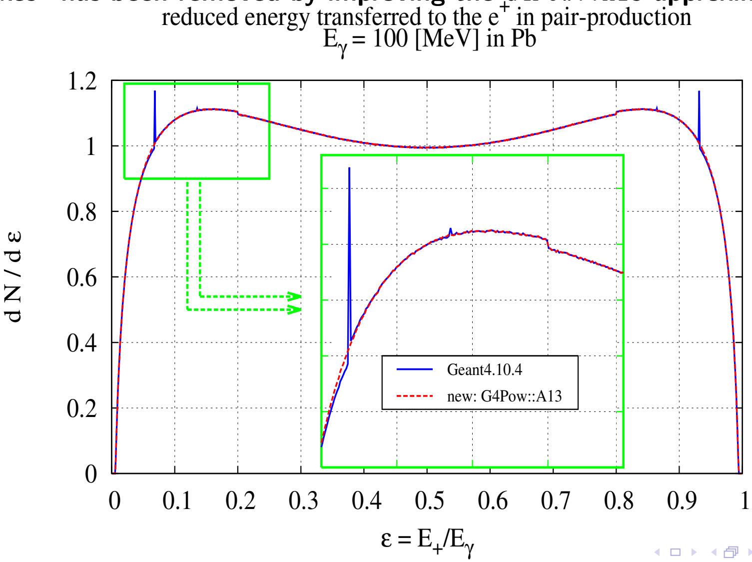

Screening: Bethe-Heitler DCS (without any corrections)

- first-order Born approximation, conversion in the field of a point-like nucleus screened by the atomic electrons
- after integrating all angular variables ($\epsilon \equiv E_+/E_\gamma, \mu \equiv m_e c^2, \delta \equiv q_{\text{min}}$)

$$\frac{\mathrm{d}\sigma}{\mathrm{d}\epsilon} = \alpha r_0^2 Z^2 \left\{ [\epsilon^2 + (1-\epsilon)^2] \left[4 \int_\delta^\mu \frac{(q-\delta)^2}{q^3} \left(1 - \frac{F(q,Z)}{Z}\right)^2 \mathrm{d}q + 4 \right] - \frac{2}{3}\epsilon(1-\epsilon) \left[4 \int_\delta^\mu \frac{q^3 - 6\delta^2 q \ln\frac{q}{\delta} + 3\delta^2 q - 4\delta^3}{q^4} \left(1 - \frac{F(q,Z)}{Z}\right)^2 \mathrm{d}q + \frac{10}{6} \right] \right\}$$

- these remaining integrals can be evaluated only numerically because of the atomic form factor $F(q,Z)$
- the atomic form factor is the Fourier transform of the atomic electron density $\rho(\vec{r})$ (spherically symmetric one)

$$F(q,Z) = \int \rho(\vec{r}) e^{i\vec{q}\vec{r}} \mathrm{d}^3 r = 4\pi \int_0^\infty \rho(r) \frac{\sin(qr)}{qr} r^2 \mathrm{d}r$$

- one can introduce the screening functions

$$\varphi_1(\delta) = 4 \int_\delta^\mu \frac{(q-\delta)^2}{q^3} \left(1 - \frac{F(q,Z)}{Z}\right)^2 \mathrm{d}q + 4 + \frac{4}{3}\ln(Z)$$

$$\varphi_2(\delta) = 4 \int_\delta^\mu \frac{q^3 - 6\delta^2 q \ln\frac{q}{\delta} + 3\delta^2 q - 4\delta^3}{q^4} \left(1 - \frac{F(q,Z)}{Z}\right)^2 \mathrm{d}q + \frac{10}{3} + \frac{4}{3}\ln(Z)$$

Screening: coherent

- using the Thomas-Fermi model of the atom, $F(q,Z)/Z$ depends only on $qZ^{-1/3}$ which makes possible to introduce Z independent $\varphi_1(\gamma)^{TF}, \varphi_2(\gamma)^{TF}$ with $\gamma \equiv 200\delta Z^{-1/3}/mc^2$
- $\varphi_1(\gamma), \varphi_2(\gamma)$ were computed numerically by using the numerical Thomas-Fermi atomic potential
- new, more accurate approximation to the universal $\varphi_1(\gamma), \varphi_2(\gamma)$ screening function were derived ($\delta \equiv 1.36\gamma$)

$$
\begin{array}{lllll}
\text{if} & \delta \leq 1.4 & \varphi_1(\delta) & = & 20.806 - 3.190\delta + 0.5710\delta^2 \\
 & & \varphi_2(\delta) & = & 20.234 - 2.126\delta + 0.0903\delta^2 \\
\text{if} & \delta > 1.4 & \varphi_1(\delta) & = & \varphi_1(\delta) = 21.019 - 4.145\ln[\delta + 0.958]
\end{array}
$$

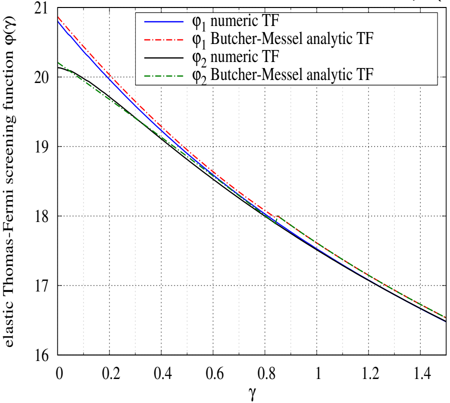

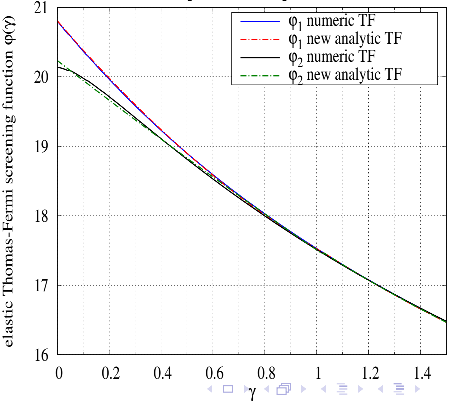

Using this new analytical approximation to the universal(TF) coherent screening functions:

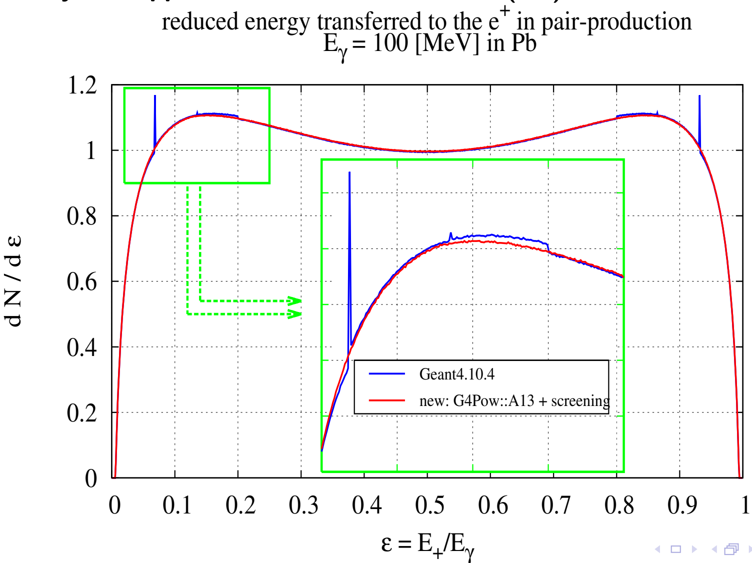

Incoherent screening functions:

- our models contain corrections to the neglected(in BH DCS) conversion in the field of atomic electrons
- the incoherent screening (by the other electrons and the nucleus) functions are similar to the coherent one

$$\psi_1(\delta) = 4\left[1 + \int_\delta^\mu \frac{(q-\delta)^2}{q^3}\frac{S(q,Z)}{Z}\mathrm{d}q\right] + \frac{8}{3}\ln(Z)$$

$$\psi_2(\delta) = 4\left[\frac{5}{6} + \int_\delta^\mu \frac{q^3 - 6\delta^2 q\ln\frac{q}{\delta} + 3\delta^2 q - 4\delta^3}{q^4}\frac{S(q,Z)}{Z}\mathrm{d}q\right] + \frac{8}{3}\ln(Z)$$

- the incoherent scattering function, $S(q,Z)$ plays the role of the atomic form factor $F(q,Z)$ now
- $S(q,Z)$ is relatively easy to compute in the Thomas-Fermi model but more involved in case of more sophisticated atomic models(see later)
- using the Thomas-Fermi model of the atom, $S(q,Z)/Z$ depends only on $qZ^{-2/3}$, which makes possible to introduce Z independent $\psi_1(\epsilon)^{TF}, \psi_2(\epsilon)^{TF}$ with $\epsilon \equiv 200\delta Z^{-2/3}/mc^2$
- $\psi_1(\epsilon), \psi_2(\epsilon)$ were computed numerically by using the numerical Thomas-Fermi atomic potential

Numerical Dirac-Fock computations:

- the Thomas-Fermi model of the atom doesn't work well in case of small Z
- more sophisticated atomic model need to be used ($\rightarrow$ we lose the universal, Z independent property of the TF model based screening)
- the DBSR_HF[1] general Dirac-Hartree-Fock program was used to compute accurate Dirac-Fock one electron orbitals for $Z = 1 - 103$
- these numerical one-electron orbitals were used to compute the corresponding atomic electron density and the Dirac-Fock atomic form factors $F(q, Z)$
- similarly, the orbitals were used to compute the Dirac-Fock incoherent scattering functions $S(q, Z)$:
  - $S(E, \theta, Z) = \sum_i^{\text{all shells}} f_i \Theta(E - U_i) n_i(p_i^{\text{max}})$
  - $n_i(p_z) \equiv \int_{-\infty}^{p_z} J_i(p_z')\mathrm{d}p_z'$
  - the one-electron Compton profile of the i-th shell: $J_i(p_z) \equiv \int\int \rho_i(\mathbf{p})\mathrm{d}p_x\mathrm{d}p_y$ which with spherical symmetry $J_i(p_z) = \frac{1}{2}\int_{p_z}^{\infty} \rho_i(p)p\mathrm{d}p$
  - the momentum distribution $\rho_i(\mathbf{p}) \equiv |\phi_i(\mathbf{p})|^2$ where $\phi_i(\mathbf{p})$ is the momentum representation of the one electron wave function $\phi_i(\mathbf{r})$
  - as a side product of this computation, Dirac-Fock one-electron momentum distributions and Compton profiles were obtained that can be used for an accurate Compton scattering model

[1] O. Zatsarinny and C. F. Fischer - Computer Physics Communications, vol. 202, pp. 287-303, 2016.

Coherent and incoherent screening functions: Thomas-Fermi vs Dirac-Fock

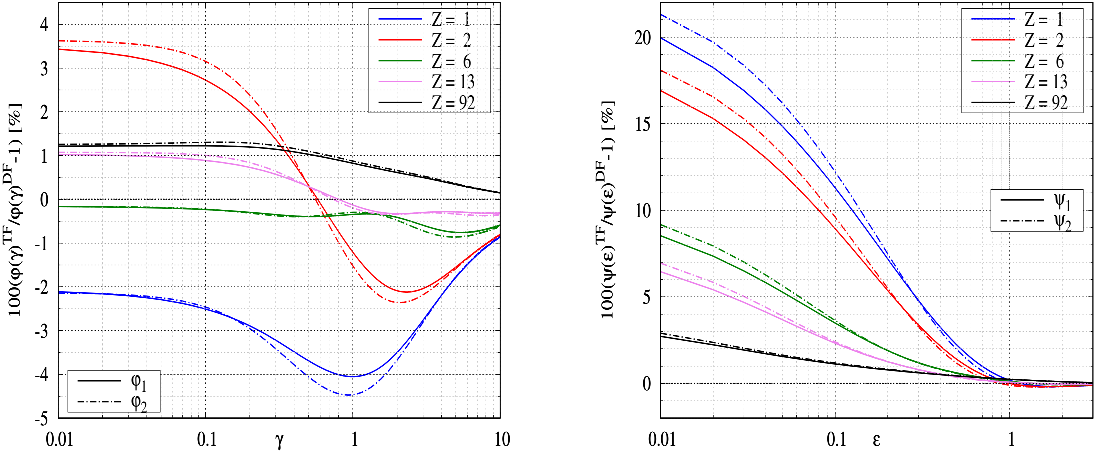

The complete screening approximation is used for low Z:

- the coherent radiation logarithm: $L_{\text{el}} \equiv \varphi_1(\gamma=0)/4 - \frac{1}{3}\ln(Z) \to L_{\text{el}}(\delta=0) = \int_\delta^\mu \frac{(q-\delta)^2}{q^3}\left(1-\frac{F(q,Z)}{Z}\right)^2 \mathrm{d}q + 1$ and $\varphi_1(0)-\varphi_2(0) = 2/3$ which in the Thomas-Fermi model $L_{\text{el}} = \ln[184.15Z^{-1/3}]$
- the coherent radiation logarithm: $L_{\text{inel}} \equiv \psi_1(\epsilon=0)/4 - \frac{2}{3}\ln(Z) \to L_{\text{inel}}(\delta=0) = \int_\delta^\mu \frac{(q-\delta)^2}{q^3}\frac{S(q,Z)}{Z}\mathrm{d}q + 1$ and $\psi_1(0)-\psi_2(0) = 2/3$ which in the Thomas-Fermi model $L_{\text{inel}} = \ln[1194Z^{-2/3}]$

New Dirac-Fock(DF) Radiation Logarithms(compared to Tsai's values)

Coherent

Z	1	2	3	4	5	6	7
L_{el}^{1}	5.310	4.790	4.740	4.710	4.680	4.620	4.570
$L_{\text{el}}^{\text{DF}}$	5.310	4.793	4.740	4.711	4.669	4.613	4.552

Incoherent

L_{inel}^{1}	6.144	5.621	5.805^{i}	5.924^{i}	6.012^{TFM}	5.891^{TFM}	5.788^{TFM}
$L_{\text{inel}}^{\text{DF}}$	5.917	5.612	5.538	5.473	5.417	5.369	5.324

[1] YS Tsai - Reviews of Modern Physics, 46(4), 815, (1974); (best estimate)

G4BetheHeitlerModel, G4PairProductionRealModel new versions in Geant4.10.5.beta:

- more robust and coherent model with improved screening correction
- numerical Dirac-Fock coherent and incoherent screening functions → possibility to produce more accurate, numerical DCS (also for bremsstrahlung)
- numerical Dirac-Fock one-electron momentum distributions, Compton profiles as side products → can be re-used for an accurate impulse approximation based Compton model
- improved and more efficient LPM correction in case of G4PairProductionRealModel
- corrected inefficient use of EM target element selector
- code cleanup and in-code documentation

Speed-up (compared to the original version)

Model	Pb Target	$PbWO_4$ Target
G4BetheHeitlerModel	11-12 [%]	25-28 [%]
G4PairProductionRealModel	10-12 [%]	290-425 [%]

Contents

`G4eBremsstrahlungRelModel` ($\leq$ `Geant4.10.5.beta`):

- based on Tsai's[1] form of the bremsstrahlung DCS, which is a Bethe-Heitler DCS with screening(TF model) and Coulomb(Bethe-Maximon) corrections to the first Born approximation
- photon emission in the field of atomic electrons is explicitly included (similarly to Wheeler and Lamb[2])
- used at $E_{e^{+/-}} > 1$[GeV]: both LPM and dielectric suppressions are included

New version of `G4eBremsstrahlungRelModel` ($>$ `Geant4.10.5.beta`):

- improved and more efficient LPM correction
- more efficient angular generator
- code cleanup and in-code documentation

[1] YS Tsai - Reviews of Modern Physics, 46(4), 815, (1974); [2] JA Wheeler, WE Lamb Jr - Physical Review, 55(9), 858, (1939)

G4SeltzerBergerModel ($\leq$ Geant4.10.5.beta):

- based on the numerical, Seltzer-Berger DCS[1], that is a synthesis of various theoretical results
- used at $E_{e^{+/-}} < 1$[GeV]: dielectric suppression is included
- rejection based sampling of emitted photon energy with *heuristic estimate* of function maximum
- 2D run-time interpolation of the numerical DCS during the final state sampling
- all these make the current model sub-optimal

New version of G4SeltzerBergerModel ($>$ Geant4.10.5.beta):

- option to use pre-prepared, Z-dependent sampling tables for faster photon energy generation
- challenging: emitted photon energy distribution has material (dielectric suppression), gamma production threshold and particle type (correction to e^+) dependence
- all these corrections can be included in a rejection loop on top of the sampling tables: very low rejection rate $\rightarrow$ high efficiency
- some memory is taken by the sampling tables (master only; 6 [MB] in case of CMS geometry)

[1] SM Seltzer, MJ Berger - NIMB, 12(1), 96, (1985)

New version of `G4SeltzerBergerModel` (> `Geant4.10.5.beta`): all corrections are included

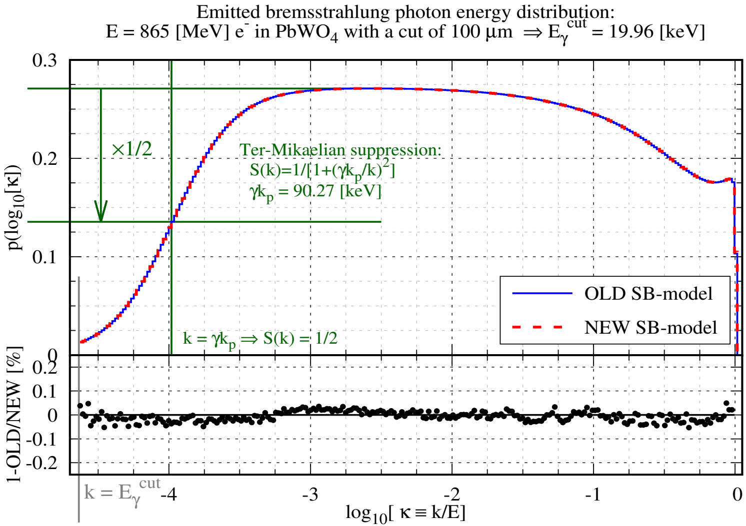

New version of `G4SeltzerBergerModel` (> `Geant4.10.5.beta`): speedup

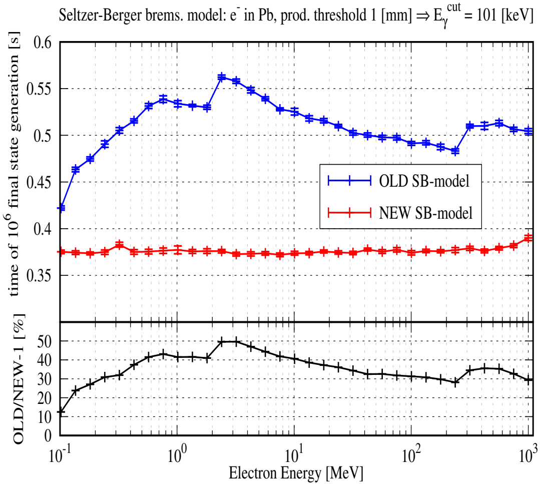

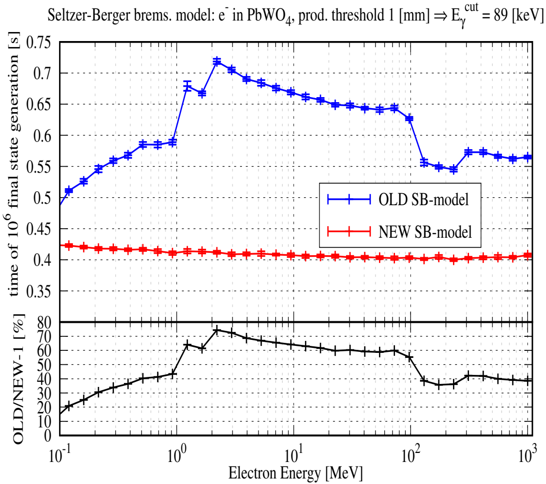

New version of G4SeltzerBergerModel, G4eBremsstrahlungRelModel (> Geant4.10.5.beta)

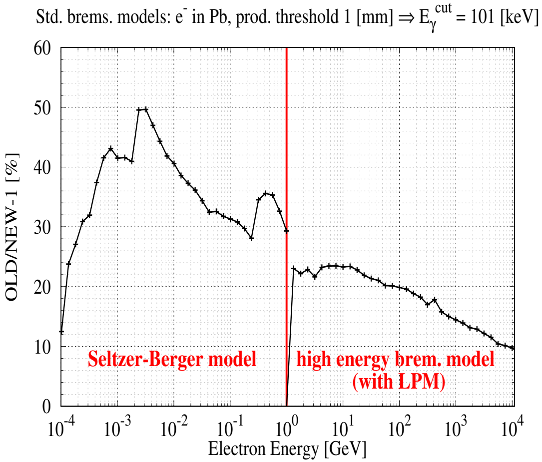

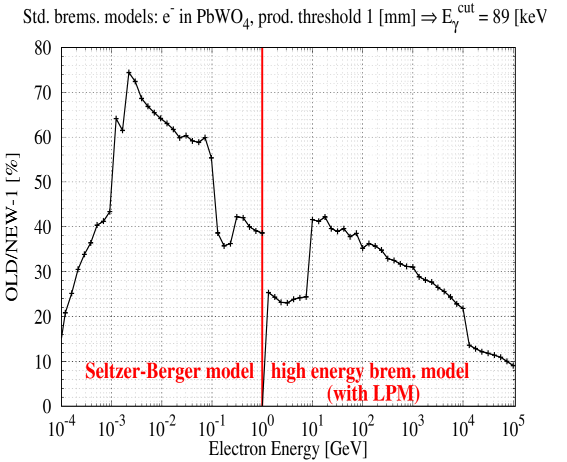

Contents

Contents

G4EmElementSelector:

- the G4VEmModel base class provides the possibility to (automatically)build a collection of G4EmElementSelector-s for each material cuts couple
- this collection can be used by the derived model at run-time, to sample the target atom of the given interaction (in case of multi-element materials)
- each individual (i.e. for a given *model* given *material* cuts couple) G4EmElementSelector of the collection stores a table of discrete probabilities of having the given interaction on a given element of the material (i.e. $P(Z_i) = \Sigma_{Z_i}/\Sigma$) over a discrete energy grid: equally spaced in log energy scale
- the implementation of the table is a vector of G4PhysicsLogVector pointer (as many as elements in the given material)
- at run-time, the target atom is sampled according to this discrete probability distribution: the probabilities are interpolated for the given primary energy
- however, **the energy bin index is re-computed for each possible target element of the material during the interpolation(at each final state sampling): just because they stored as individual log-vectors**
- each of these re-computation means a (redundant) computation of the logarithm of the primary particle kinetic energy, that can be skipped

Contents

Storing the logarithm of the primary particle kinetic energy:

- the most optimal and re-usable solution to the G4EmElementSelector problem: having the logarithm of the primary particle kinetic energy + caching the last energy bin index that was used
- logarithm of the kinetic energy can be stored and updated together with the kinetic energy (in G4DynamicParticle to guarantee consistency!)
- the logarithm of the kinetic energy can be re-used to speed-up table interpolations: dE/dx, range, lambda table interpolations at run-time
- several redundant computations of the log-kinetic energy can be skipped at each step → reduce the cost of G4PhysicsVector::Value: all those tables are G4PhysicsLogVector-s i.e. values over the primary particle kinetic energy spaced equally in log scale

```
inline void G4DynamicParticle::SetKineticEnergy(G4double aEnergy)
{
    isLogEkinUpToDate = ( isLogEkinUpToDate && (theKineticEnergy == aEnergy) );
    theKineticEnergy  =  aEnergy;
}
```

```
inline G4double G4DynamicParticle::GetLogKineticEnergy() const
{
  if (!isLogEkinUpToDate) {
    theLogKineticEnergy = (theKineticEnergy>0.) ? G4Log(theKineticEnergy) : -42.;
    isLogEkinUpToDate   = true;
  }
  return theLogKineticEnergy;
}
```

10 [GeV] e^- in Simplified Sampling Calorimeter: 50 layers of 2.3 [mm] Pb and 5.7 [mm] liquid-Ar

CURRENT: re-compute Log(kinetic energy)

Incl.	Self	Called	Function
10.19	0.80	43 584 415	G4PhysicsVector::Value(double, unsigned long&) co...

===

Incl.	Self	Called	Function
6.92	2.18	57 535 356	G4Log(double)

****** ~23 % reduction in calls to `G4Log()` → few % run-time improvement ******

NEW: stored Log(kinetic energy)

Incl.	Self	Called	Function
5.52	0.65	33 166 475	G4PhysicsVector::Value(double, double, unsigned long&) c...
2.60	0.20	10 417 940	G4PhysicsVector::Value(double, unsigned long&) const

===

Incl.	Self	Called	Function
5.39	1.70	44 529 120	G4Log(double)

Proposition:

- the solution proposed (see the code in the previous slide) guarantee, that the logarithm of the kinetic energy is computed only on demand and re-computed only if it's necessary
- the corresponding modifications(usually very small, see above) affects several categories (`particles`, `global`, `emutils`, `emstand`)
- these modifications can be applied in a dedicated `git branch` on top of a well defined base
- the usual *Geant4 Profiling and Benchmarking* can be done (*Julia&Soon*) and further actions can be taken based on the results
- note, that the proposed modifications:
    - do not change the simulation results (i.e. numerically identical results)
    - practically zero run-time overhead (`isLogEkinUpToDate = false` by default)
    - one additional `double` and a `boolean` member in `G4DynamicParticle`
    - it should give $\sim$ few % run-time improvement and $\sim$23 % reduction in calls to `G4Log()`

Contents

Summary:

- the Goudsmit-Saunderson MSC model with its spin-relativistic correction and error-free stepping options provides an accurate model for $e^{-}/+$ Coulomb scattering from low to high Z materials down to $\sim$ keV energies
- a detailed $e^{-}/+$ transport benchmark against experimental data is ongoing in order to demonstrate this
- standard (and non-standard) bremsstrahlung and pair-production models have been improved both in terms of accuracy and spped
- these computations provided ingredients that can be used in the future for further model improvements
- an optimisation of the EM framework is suggested by significantly reducing the number of calls to `G4Log()` while keeping the results numerically identical